Modulated optical transmission of subwavelength hole arrays in metal-VO_2 films

J. Y. Suh,[a] E. U. Donev, R. Lopez, L. C. Feldman, and R. F. Haglund, Jr.
Department of Physics and Astronomy and Vanderbilt Institute of Nanoscale Science and Engineering, Vanderbilt University, Nashville, Tennessee 37235

(Received 4 October 2005; accepted 2 March 2006; published online 29 March 2006)

We demonstrate the modulation of the transmission of near-infrared light through a periodic array of subwavelength apertures in Ag–VO_2 and Au–VO_2 double-layer films using the semiconductor-to-metal phase transition in VO_2. The transmitted intensity ratio increases by a factor of 8 as the VO_2 goes from the semiconductor to the metal phase. We attribute this modulation to the switchable dielectric-permittivity contrast between the air-filled holes in the array and the surrounding VO_2 material, a conjecture that is semiquantitatively confirmed by simulation. © *2006 American Institute of Physics*. [DOI: 10.1063/1.2190463]

Enhanced optical transmission (EOT) through subwavelength hole arrays in optically thick metal films has been proposed as a way to transmit light through nanostructures.[1,2] Ordered arrays of nanoapertures and similar nanostructures have been considered as field enhancers and controllers for near-field electromagnetic waves.[3,4] In all such applications modulation of the EOT effect would be required for active control. Here we demonstrate a temperature-controlled modulation of the EOT effect in a nanostructured bilayer film by means of the semiconductor-to-metal transition (SMT) in vanadium dioxide.

In a typical EOT experiment, the subwavelength hole array in a film covers a transparent solid substrate; the characteristics of the transmission spectra are fixed by the dielectric constants of the materials that bound the array and by the hole depth and pitch.[5,6] Kim *et al.*[7] have constructed a switchable structure comprising a liquid crystal layer sandwiched between a transparent indium-tin-oxide electrode and a perforated chromium film on quartz; modulation, albeit at relatively slow speeds, is achieved by varying the applied electric field. In a contrasting approach, the reflectivity of a propagating surface plasmon polariton, modulated by heating to induce the transformation from the α phase to a metallic liquidlike phase in gallium, has been implemented by Krasavin *et al.* in an attenuated total-reflection geometry.[8]

In our approach, pictured in Fig. 1(a), the transmission of light incident on a nanohole array in a metal film is modulated by switching an underlying VO_2 layer between metallic (m-VO_2) and semiconducting (sc-VO_2) phases with distinctly different dielectric functions, particularly in the infrared.[9,10] Here the SMT is induced thermally at a critical temperature near 70 °C, but could be triggered on a femtosecond time scale by laser irradiation.[11] The transmission enhancement takes place in the VO_2 metallic phase, a surprising result given that the transmissivity of m-VO_2 is substantially less than that of sc-VO_2 for unstructured VO_2 films. This "reverse optical switching," in which the transmission behaves opposite to that of an unperforated VO_2 film, is explained in a simple model and numerical simulations that give a qualitative explanation for the experimental findings.

The double-layer structure of Fig. 1(a) was produced in two steps. A 200 nm thick VO_2 film was grown on a fused silica substrate by pulsed laser deposition.[12] Then Ag and Au overlayers substantially thicker than the optical skin depth (160 and 230 nm for Ag and Au, respectively) were thermally evaporated onto the VO_2 film. The stoichiometry and thickness of each film were confirmed by Rutherford backscattering spectrometry. A 30 keV Ga^+ focused ion beam was then used to mill a square array of nominally cylindrical apertures, with a diameter $d=300$ nm for Ag–VO_2 and $d=240$ nm for Au–VO_2; the array pitch was 750 nm for both structures. Figure 1(b) shows light passing through the Ag–VO_2 array, as imaged in illumination mode ($\lambda=532$ nm) by a scanning near-field optical microscope

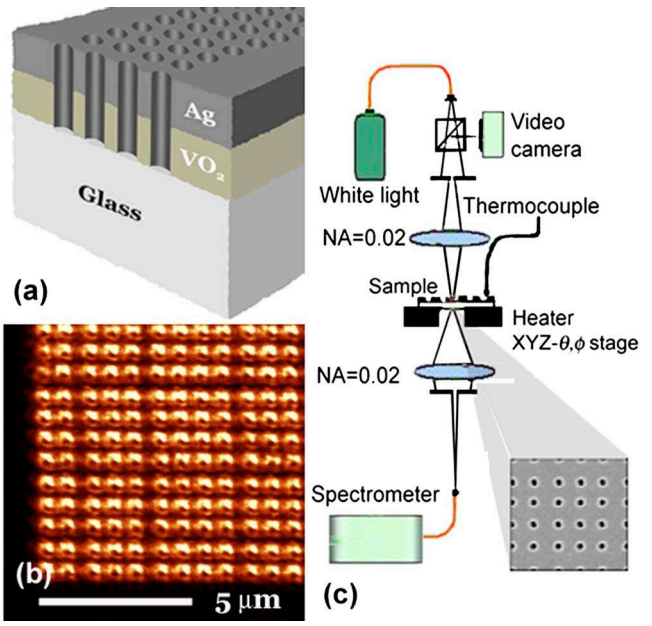

FIG. 1. (Color online) (a) Schematic drawing of subwavelength hole array structure in metal-VO_2 double-layer film on silica substrate, where the metal may be either Ag or Au. (b) Scanning near-field optical microscope (SNOM) image of the 50×50 μm^2 Ag–VO_2–silica hole array of 240 nm diameter and 750 nm pitch in the high-temperature phase of VO_2 middle layer. The brightness in color stands for a stronger intensity in the far-field collection optics. (c) Schematic of the experimental setup used for optical transmission measurements.

[a]Electronic mail: jae.y.suh@vanderbilt.edu

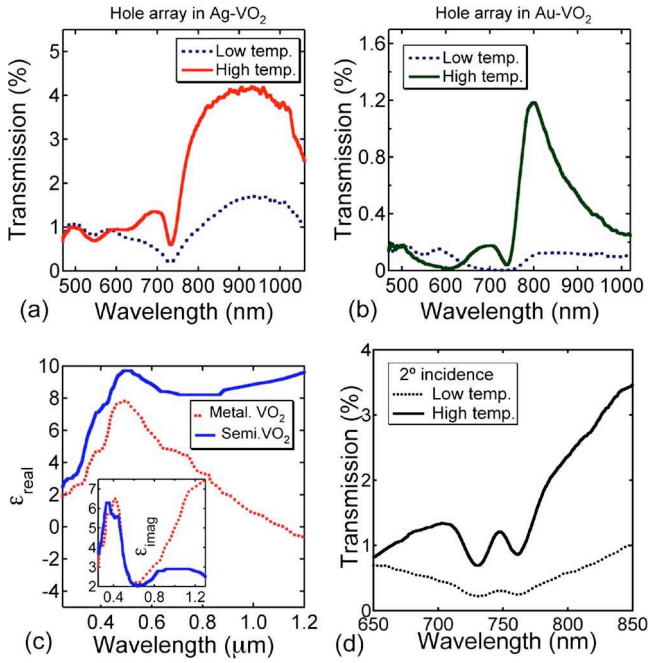

FIG. 2. (Color online) (a) Zeroth-order transmission of $Ag-VO_2$–silica hole array with a diameter of 300 nm and a lattice constant of 750 nm. The solid line was obtained in the metallic phase of VO_2 middle layer, while the dotted line was acquired in the semiconducting phase. (b) Transmission of $Au-VO_2$–silica sample; the solid and dashed lines have the same meaning as in (a). (c) The real part of the dielectric functions of VO_2 in the visible range. The inset represents the imaginary part of the dielectric functions. (d) Transmission spectra for 2° tilted incident angle in the high- and low-temperature states of a $Ag-VO_2$–silica hole array: the Rayleigh wavelengths $\lambda(R)$ for grazing orders should become longer for angles on one side of the sample and shorter for angles on the other side with increasing incident angle. The sharp minimum at $\lambda(R)$ splits into one occurring at $\lambda(R-)<\lambda(R)$ and the other at $\lambda(R+)>\lambda(R)$.

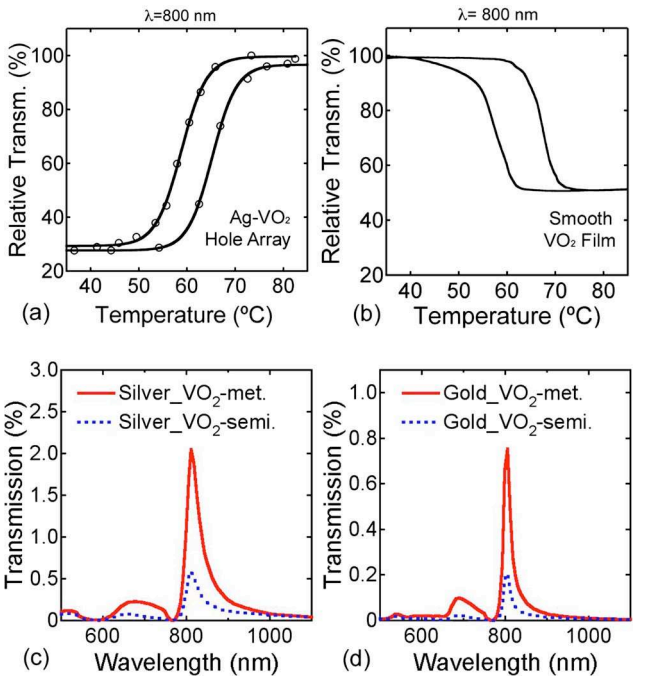

FIG. 3. (Color online) (Top line) Transmission hysteresis curves as a function of temperature at $\lambda=800$ nm obtained from the $Ag-VO_2$ double-layer hole array (a) and a smooth 200 nm thick VO_2 film on silica (b). (Bottom line) Results of simulations for zeroth-order transmission for (c) $Ag-VO_2$–silica and (d) $Ag-VO_2$–structures.

(SNOM, aperture diameter $\approx$100 nm). The sample was mounted on a heated three-dimensional translation-rotation stage equipped with a precision thermocouple, shown in Fig. 1(c). The far-field transmission T_{00} in the visible and near IR was measured by focusing a white-light source incident through the sample. The transmitted far-field light was collected by a microscope objective, aligned with the incident beam within a 1° angle, coupled to a multimode optical fiber leading to a monochromator equipped with a cooled-CCD detector (CCD denotes charge-coupled device).

Figures 2(a) and 2(b) show the EOT spectra for the $Ag-VO_2$ and $Au-VO_2$ hole array at temperatures corresponding to the semiconducting and metallic phases of VO_2. The most striking feature is a significant increase of the transmitted intensity in the near IR when the VO_2 becomes metallic, while the transmission difference between the two VO_2 phases in the visible range is relatively small. As shown in the Fig. 2(c), the dielectric functions differ substantially only for wavelengths greater than approximately 600 nm,[10] suggesting that the wavelength dependence of the VO_2 dielectric function controls the switching effect. The contrast ratio at $\lambda=800$ nm in T_{00} for m-VO_2 and sc-VO_2 is $\sim$8 for the $Au-VO_2$ hole array and $\sim$3 for the $Ag-VO_2$ hole array. The absolute value of T_{00} for the $Au-VO_2$ structure, however, is only one-third of that for the $Ag-VO_2$ structure, due to the larger Au layer thickness[6] and the smaller hole effective diameter.[13] The $Au-VO_2$ structure has a narrower transmission peak than the $Ag-VO_2$ structure, as expected from the electromagnetic coupling of the incident light to surface plasmon polaritons. The relatively smaller holes in the $Au-VO_2$ structure scatter the surface modes less efficiently into far-field light, diminishing the radiative damping and increasing the lifetime of these modes.[14]

The sharp normal-incidence minima at 740 nm [Figs. 2(a) and 2(b)], corresponding to the nominal lattice spacing of the hole arrays, are identifiable as the nonresonant Wood's anomaly for diffraction gratings.[15] Figure 2(d) shows transmission as a function of wavelength and temperature near the position of the Wood's anomaly when the sample is tilted 2° from the optical axis. The fact that the Wood's anomaly is not split in the data of Figs. 2(a) and 2(b) indicates that the sample is properly aligned and that the zeroth order or direct transmission through the hole array is what is being measured.

The hysteresis in T_{00} for the $Ag-VO_2$ array as a function of temperature at a wavelength of 800 nm is shown in Fig. 3(a). The transmission function is just the reverse of that measured for an unstructured VO_2 film [Fig. 3(b)]. Hence it can be inferred that the light impinging on the metal-VO_2 holes is transmitted by a different mechanism. The SNOM scan in Fig. 1(b) shows that the transmitted light is mainly localized in the holes and that no light traverses the unperforated region of the double-layer structure. Thus, the hole array receives the same amount of evanescent wave regardless of the VO_2 phase. However, some fraction of the evanescent wave entering the holes in the VO_2 can penetrate the sidewalls. In this case, light will be channeled out of the zeroth-order transmission path differently, depending upon the VO_2 phases. In addition, the waves emerging from the holes in the metal may undergo further scattering at the VO_2-silica interface.

A simple model based on the contrast in dielectric functions between the metallic and semiconducting states ac-

counts for the key features of this behavior. The amount of light that leaks and scatters into the VO_2 material and the silica substrate is determined by the permittivity contrast between the hole (air) and its surroundings (VO_2). Lower permittivity contrast reduces both the leakage into the VO_2 layer and the diffuse scattering at the VO_2-silica interface.[16] In the visible spectrum, the permittivity contrast between the two phases is small, as shown in Fig. 2(c). However, in the near IR, $\varepsilon_{\text{real}}$ (m-VO_2) differs significantly from $\varepsilon_{\text{real}}$ (sc-VO_2) and approaches the values for silica; for example, at 850 nm $\varepsilon(\text{m-VO}_2)=2.67+2.98i$, while $\varepsilon(\text{sc-VO}_2)=8.17+2.65i$. Hence the SMT enhances the zeroth-order transmission by reducing the contrast between the holes and their surroundings.

Calculations of T_{00} based on a plane-wave decomposition and a transfer matrix formalism[17] confirm the general features of the EOT results, as shown in Figs. 3(c) and 3(d). The simulations use the optical constants of VO_2 extracted from Ref. 10 and for Ag and Au taken from Ref. 18. The calculated spectra reproduce the factor of 3 difference in T_{00} for the Au–VO_2 compared to Ag–VO_2 structures; they exhibit the larger relative width of the T_{00} spectrum for Ag–VO_2; and most importantly, they confirm the existence of the reverse switching effect in the near IR. However, computational studies suggest that much larger numbers of plane waves are needed to adequately represent structures of this complexity.[19]

In conclusion, we have demonstrated that the extraordinary optical transmission through subwavelength hole arrays in Ag–VO_2 and Au–VO_2 bilayer structures can be modulated by reversibly switching the VO_2 layer between the metallic and semiconducting phases. This counterintuitive effect is explained by a simple model in which the losses in the zeroth-order transmission are caused by light leaking into the VO_2 layer and diffuse scattering at the exit apertures. The loss of transmitted intensity increases with higher permittivity contrast between the interior and the exterior of the holes, which can be controlled by the VO_2 phase transition. Optical modulation using this system can be envisioned, since the semiconductor-to-metal transition has been shown to be as fast as 100 fs,[20] while the speed of the metal-to-semiconductor transition will be determined by thermal design.[21]

The authors thank A. B. Hmelo for helpful discussions on FIB fabrication and F. Villegas and P. B. Gray for their assistance with the SNOM imaging. This research was supported by the U. S. Department of Energy (Nanoscale Science, Engineering and Technology program, DE-FG02-01ER45916) and by a National Science Foundation Nanoscale Integrated Research Team (NIRT) through Project No. DMR-0210785.

[1] T. W. Ebbesen, H. J. Lezec, H. F. Ghaemi, T. Thio, and P. A. Wolff, Nature (London) **391**, 667 (1998).
[2] H. F. Ghaemi, T. Thio, D. E. Grupp, T. W. Ebbesen, and H. J. Lezec, Phys. Rev. B **58**, 6779 (1998).
[3] M. Salerno, J. R. Krenn, B. Lamprecht, G. Schider, H. Ditlbacher, N. Felidj, A. Leitner, and F. R. Aussenegg, Opto-Electron. Rev. **10**, 217 (2002).
[4] W. L. Barnes, A. Dereux, and T. W. Ebbesen, Nature (London) **424**, 824 (2003).
[5] S. A. Darmanyan and A. V. Zayats, Phys. Rev. B **67**, 35424 (2003).
[6] A. Degiron, H. J. Lezec, W. L. Barnes, and T. W. Ebbesen, Appl. Phys. Lett. **81**, 4327 (2002).
[7] T. J. Kim, T. Thio, T. W. Ebbesen, D. E. Grupp, and H. J. Lezec, Opt. Lett. **24**, 256 (1999).
[8] A. V. Krasavin, A. V. Zayats, and N. I. Zheludev, J. Opt. A, Pure Appl. Opt. **7**, S85 (2005).
[9] F. J. Morin, Phys. Rev. Lett. **3**, 34 (1959).
[10] H. W. Verleur, A. S. Barker, and C. N. Berglund, Phys. Rev. **172**, 788 (1968).
[11] M. Rini, A. Cavalleri, R. W. Schoenlein, R. Lopez, L. C. Feldman, R. F. Haglund, L. A. Boatner, and T. E. Haynes, Opt. Lett. **30**, 558 (2005).
[12] J. Y. Suh, R. Lopez, L. C. Feldman, and R. F. Haglund, Jr., J. Appl. Phys. **96**, 1209 (2004).
[13] K. L. van der Molen, F. B. Segerink, N. F. van Hulst, and L. Kuipers, Appl. Phys. Lett. **85**, 4316 (2004).
[14] D. S. Kim, S. C. Hohng, V. Malyarchuk, Y. C. Yoon, Y. H. Ahn, K. J. Yee, J. W. Park, J. Kim, Q. H. Park, and C. Lienau, Phys. Rev. Lett. **91**, 143901 (2003).
[15] M. Sarrazin, J. P. Vigneron, and J. M. Vigoureux, Phys. Rev. B **67**, 85415 (2003).
[16] W. Bogaerts, P. Bienstman, D. Taillaert, R. Baets, and D. De Zutter, IEEE Photonics Technol. Lett. **13**, 565 (2001).
[17] S. G. Tikhodeev, A. L. Yablonskii, E. A. Muljarov, N. A. Gippius, and T. Ishihara, Phys. Rev. B **66**, 45102 (2002).
[18] E. D. Palik, *Handbook of Optical Constants of Solids* (Academic, Orlando, 1985).
[19] A. Christ, S. G. Tikhodeev, N. A. Gippius, J. Kuhl, and H. Giessen, Phys. Rev. Lett. **91**, 183901 (2003).
[20] A. Cavalleri, T. Dekorsy, H. H. W. Chong, J. C. Kieffer, and R. W. Schoenlein, Phys. Rev. B **70**, 161102 (2004).
[21] E. Sovero, D. Deakin, J. A. Higgins, DeNatale, and S. Pittman, Proceedings of the IEEE GaAs IC Symposium (IEEE, New York, 1990), p. 101.